

Role of ^{18}F -fluorodeoxyglucose positron emission tomography/computed tomography and magnetic resonance imaging in prediction of response to neoadjuvant chemotherapy in pediatric osteosarcoma

ABSTRACT

The aim of our study was to evaluate the role of ^{18}F -fluorodeoxyglucose positron emission tomography/computed tomography (PET/CT) and magnetic resonance imaging (MRI) in prediction of response to neoadjuvant chemotherapy (NAC) in pediatric osteosarcoma (OS) patients compared to percentage of tumor necrosis after surgical excision of the tumor. Forty-six pediatric OS patients treated with neoadjuvant chemotherapy and surgery were underwent PET/CT and MRI before, after 3 cycles, and after the completion of neoadjuvant chemotherapy. Imaging parameters include maximum standardized uptake value (SUVmax1, 2, and 3), tumor liver ratio (TLR 1, 2, and 3), and MRI tumor volume (MRTV 1, 2, and 3) at initial assessment before starting NAC, after finishing three cycles and after finishing 6 cycles before tumor excision, respectively. Cutoff values of the PET/CT and MRI parameters were determined using receiver operating characteristic (ROC) curve analysis and percentage of tumor necrosis of postsurgical specimen. Fourteen patients were good responders (30.4%), with more than 90% tumor necrosis, while 31 patients were poor responders (67.4%). The results of one patient were missed. We noticed that higher sensitivity for detecting poor responders was detected by SUVmax3/1, TLR3/1, and MRTV2/1 ratio cutoff values, while higher specificity was detected by TLR2 and SUVmax3 cutoff values. ROC curve analysis of MRTV2/1 and MRTV3/1 ratio was fair in predicting poor responders. PET/CT parameters are capable of predicting histological response to NAC in OS patients with overall sensitivity and specificity higher than MRI parameters.

Keywords: ^{18}F -fluorodeoxyglucose positron emission tomography/computed tomography, magnetic resonance imaging, neoadjuvant chemotherapy, osteosarcoma

INTRODUCTION

Osteosarcoma (OS) is the most common malignant bone tumor. It arises from primitive mesenchymal bone-forming cells and its histologic hallmark is the production of malignant osteoid.^[1]

Most patients with OS present with pain and swelling in the involved region and usually seek medical advice following trauma or vigorous physical exercise.^[2]

Although OS can occur in any bone, it is most common in the metaphysis of the long bones. The most common primary sites are the distal femur, proximal tibia, and proximal humerus.

However, since about 80% of patients with localized OS develop metastatic disease following surgical resection,

**JEHAN AHMED YOUNIS, ISMAEL MOHAMMED AL ANTABLY¹,
MANAL ZAMZAM², HALA TAHA SALEM³,
EMAN MOHAMMED ZAKI⁴, OMNEYA AHMED HASSANIAN⁵**

Department of Oncology and Nuclear Medicine, Faculty of Medicine, Cairo University, Departments of ¹Nuclear Medicine, ²Pediatric Oncology, ³Pathology, ⁴Radiology and ⁵Statistics, National Cancer Institute, Children Cancer Hospital, Cairo, Egypt


Address for correspondence: Dr. Jehan Ahmed Younis, Emtedad El Amal, El Maadi, Cairo, Egypt.
E-mail: jehan.nuc@hotmail.com

Submission: 15-05-2018 **Accepted:** 12-06-2018 **Published:** 18-12-2019

This is an open access journal, and articles are distributed under the terms of the Creative Commons Attribution-NonCommercial-ShareAlike 4.0 License, which allows others to remix, tweak, and build upon the work non-commercially, as long as appropriate credit is given and the new creations are licensed under the identical terms.

For reprints contact: reprints@medknow.com

How to cite this article: Younis JA, Al Antably IM, Zamzam M, Salem HT, Zaki EM, Hassanian OA. Role of ^{18}F -fluorodeoxyglucose positron emission tomography/computed tomography and magnetic resonance imaging in prediction of response to neoadjuvant chemotherapy in pediatric osteosarcoma. World J Nucl Med 2019;18:378-88.

Access this article online	
Website: www.wjnm.org	Quick Response Code 
DOI: 10.4103/wjnm.WJNM_52_18	

virtually all patients are presumed to have subclinical, microscopic metastases.^[3]

The most common site for metastases is the lung; however, metastases can also occur in other bones and soft tissues.

Computed tomography (CT) and magnetic resonance imaging (MRI) are the imaging procedures of choice in locoregional staging as both modalities can detect intraosseous and extraosseous spread, skip metastases, growth plate, and articular involvement. Thoracic CT is the study of choice in detecting lung metastases.^[4] MRI does not only make a significant contribution to correct local staging of OS but also assists in determining the most appropriate surgical management.

OS typically show increased uptake of radiotracer on bone scans obtained by use of technetium-99m (^{99m}Tc) methylene diphosphonate. The bone uptake is often more than the extent of the tumor due to reactive response surrounding the tumor. Therefore, it is difficult to assess the actual size of the tumor on bone scans. Skip lesions and pulmonary metastases may also concentrate the radioisotope, but skip lesions are more reliably depicted by MRI. Bone scans are most useful in excluding multifocal disease. ^{99m}Tc-sestamibi (MIBI) scintigraphy can be used to assess response to chemotherapy in OS.^[5] ¹⁸F-fluorodeoxyglucose positron emission tomography/CT (¹⁸F-FDG PET/CT) enables the assessment of glucose metabolism and also the metabolic activity of malignant tissue by calculating a standardized uptake value (SUV). Change in SUV after neoadjuvant chemotherapy has been reported to be useful in predicting tumor response in OS.^[6]

Tumor cellular necrosis fraction is considered the hallmark of treatment response to chemotherapy in sarcomas; however, overinterpretation of tumor cellular necrosis in a tumor specimen may result in cases for which necrosis was present as a distinguishing feature of the primary tumor.^[7] Some primary sarcomas show significant necrosis before therapy. For this reason, reliable treatment response imaging in sarcoma requires a baseline pretreatment scan for comparison.^[8]

The mainstay of therapy of OS is surgical removal of the malignant lesion. Most often, limb-sparing (limb-preserving) procedures can be used to treat patients with this disease and thus, preserve function. Chemotherapy is also required to treat micrometastatic disease, which is present but often not detectable in most patients (about 80%) at the time of diagnosis.^[9]

Adjuvant and neoadjuvant chemotherapy has significantly improved the long-term survival rate of patients with high-grade OS, compared with surgery alone.^[10] The current standard of chemotherapy response evaluation is to histologically assess the tumor necrosis of the excised lesion,^[11] which has been reported to be the most important prognostic factor in OS after neoadjuvant chemotherapy.^[12]

The aim of the current study was to evaluate the role of ¹⁸F-FDG PET/CT and MRI in the prediction of response to neoadjuvant chemotherapy (NAC) in pediatric OS patients after week 5 and week 10 (before local surgical control) compared to percentage tumor necrosis after surgical excision of the tumor.

MATERIALS AND METHODS

Patients criteria and study design

Prospective study for 46 patients with histologically proven OS imaged with PET/CT and MRI before and while they were under treatment at the Children Cancer Hospital, Egypt, (CCHE) during the period from October 2014 to October 2017. The study was approved by the Institutional Ethical Committee.

The age of patients in the study ranged from 5 to 17 years with a median of 13 years and a mean of (12.28 ± 0.49). The study included 26 males (56.5%) and 20 females (43.5%).

The histologically proven patients with OS were investigated by PET/CT and MRI three times; the first at initial assessment before starting the neoadjuvant chemotherapy, the second after finishing three cycles of chemotherapy, and the last after finishing 6 cycles and before tumor excision. PET/CT (SUVmax) and MRI (tumor volume) results were compared with the percentage of tumor necrosis and pathological response after surgical resection.

Only 32 patients from 46 underwent the three PET/CT and MRI scans. Eight patients underwent first and second scans and missed the third one, and six patients underwent the first and third scans and missed the second one.

¹⁸F-fluorodeoxyglucose positron emission tomography/computed tomography

¹⁸F-FDG PET/CT study was performed using a dedicated PET/CT scanner (Biograph, TruePoint; Siemens). This machine integrates a PET scanner with a dual-section helical CT scanner (40 slice Emotion; Siemens) and allows the acquisition of coregistered CT and PET images in one session.

Patient preparation

The patients were asked to fast for 4–6 h before PET/CT. Blood sugar levels were checked to ensure that there was no hyperglycemia, a level of less than 150 mg/dl is desirable. None of our patients was diabetic.

8.14 MBq/kg body weight of FDG was administered intravenously 1 h before imaging. Patients sat quietly in a dimly lit room during the uptake phase and were asked to void just before imaging. The CT and PET scans were obtained with the patient in quiet respiration. They were instructed to avoid any kind of strenuous activity 24 h before the examination to avoid physiologic muscle uptake of FDG. Forty-five to sixty minutes after FDG injection, the patients were placed supine on the imaging table acquiring at first the CT portion of the study. This was applied as whole-body scan with application of intravenous contrast (PET/CECT). A whole-body PET study (totally covering the involved tumor sites) followed an enhanced whole-body CT study. The CT study took approximately 60–70 s to be completed and the PET study was done for +2 min per bed position.

Imaging technique

Computed tomography imaging protocol

For a typical whole-body PET/CT study (neck, chest, abdomen, pelvis, and lower limbs if needed), scanning began at the level of the skull base and extended caudally to include the involved tumor site. Typical scanning parameters would be a collimator width of 3.0 mm, pitch of 1.5, gantry rotation time of 0.8 s, and field of view of 50 cm.

The resulting images from CT reconstructed with a 512 × 512 matrix and a 50-cm field of view, were converted using equivalent attenuation factors of 511 keV for attenuation correction.

Positron emission tomography imaging

PET performed on a dedicated PET scanner with approximately six to eight-bed positions that planned in the three-dimensional acquisition mode for scanning the entire patient with 2-min acquisition at each bed position in a caudocranial direction. The PET images were reconstructed with a 128 × 128 matrix, an ordered subset expectation maximum iterative reconstruction algorithm (2 iterations, 28 subsets), an 8-mm Gaussian filter, and a 50 cm field of view. Then PET, PET/CT, and CT images were reviewed using a dedicated workstation and software (E. soft; Siemens Medical Solutions), which allowed three-dimensional displays (transaxial, coronal, and sagittal) to be constructed using CT, PET, and PET/CT images and maximum intensity projection displays of the PET data.

Qualitative image interpretation with positron emission tomography and positron emission tomography/computed tomography

Accurate interpretation of FDG-PET scans requires a thorough knowledge of the normal physiologic distribution of FDG and of normal variants that may reduce the accuracy of PET studies, thereby significantly affecting patient treatment

Quantitative measurement with positron emission tomography

Standardized uptake value

The tumor SUV is a semiquantitative parameter that represents the metabolic activity in a static image as measured by region-of-interest technique and corrected for both the injected activity per kilogram of body weight and the blood glucose level.

Image interpretation

Focal FDG uptake was considered abnormal when it was greater than that of hepatic uptake, regarding the diagnosis of metastatic deposits. All PET/CT scans were reviewed and interpreted by two experienced nuclear medicine physicians.

Magnetic resonance imaging

MRI sequences included a standard (spin-echo) T1-weighted sequence (repetition time [ms]/echo time [ms], 400–900/10–20), with or without gadolinium enhancement, and an intermediate weighted/T2-weighted sequence (1500–2500/70–100), without fat suppression. Intramedullary tumor lengths were measured in coronal sections of unenhanced T1-weighted sequences, and tumor widths and depths were measured in axial enhanced T1- and T2-weighted sequences without fat suppression. All MRI images were reviewed and interpreted by two experienced radiology physicians.

Neoadjuvant chemotherapy

The treatment plan for OS cases at CCHE was demonstrated at Figure 1.

Histologic assessments of response to preoperative chemotherapy

Histologic responses to NAC were evaluated in the resected specimen by an experienced pathologist. Good response was defined as 90% or more tumor necrosis while the poor response was defined if <90% tumor necrosis was achieved.

Definitions and calculations of parameters

Prechemotherapy (initial) SUVmax and MRI tumor volume (MRTV) defined as SUVmax1 and MRTV1. Prechemotherapy (initial) tumor SUVmax to liver SUVmax ratio defined as tumor liver ratio (TLR1). Postweek 5 SUVmax and MRTV defined as

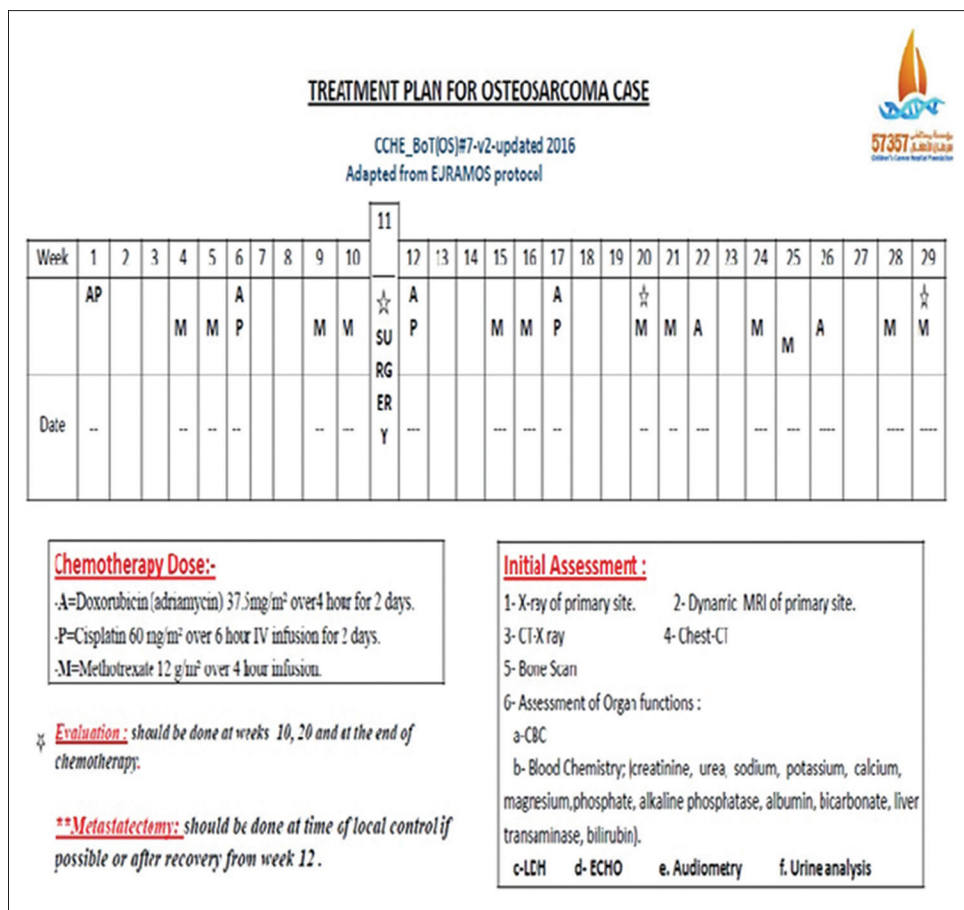


Figure 1: Protocol of osteosarcoma treatment at Children Cancer Hospital, Egypt

SUVmax2 and MRTV2. Postweek 5 tumor SUVmax to liver SUVmax ratio defined as TLR2. Postweek 10 SUVmax and MRTV defined as SUVmax3 and MRTV3. Postweek 10 tumor SUVmax to liver SUVmax ratio defined as TLR3. SUV change ratio 2/1 = SUV2/SUV1. SUV change ratio 3/1 = SUV3/SUV1. MRTV change ratio 2/1 = MRTV2/MRTV1. MRTV change ratio 3/1 = MRTV3/MRTV1. TLR change ratio 2/1 = TLR2/TLR1. TLR change ratio 3/1 = TLR3/TLR1.

Statistics

The Wilcoxon signed-rank test was used for paired comparisons between quantitative parameters. The receiver operating characteristic (ROC) curves for the prediction of a poor histologic response were generated to determine the cutoff values that offered the highest sensitivity and specificity of the PET and MRI parameters which are SUV1, SUV2, SUV3, TLR2, TLR3, SUV2/1, SUV3/1, MRTV2/1, MRTV3/1, TLR2/1, and TLR3/1, in terms of their abilities to discriminate good from poor responders. All calculations were performed using SPSS (version 22.0; SPSS Inc., Chicago, IL, USA). All P values were derived from the two-sided test, and values of <0.05 were considered statistically significant. We used related sample Wilcoxon

signed-rank test for testing change in scans at the different time points.

RESULTS

Patient characteristics

This prospective study included 46 patients with histologically proven OS who were under treatment and regular follow-up at the CCHC during the period from October 2014 to October 2017. The age of patients encountered in the study ranged from 5 to 17 years with a median of 13 years, mean of 12.28 ± 0.49. They included 26 males (56.5%) and 20 females (43.5%).

Regarding histopathology, all patients had high-grade OSs except one patient. Twenty-nine patients (62.2%) proved to be of osteoblastic type (62.2%).

According to the site of the primary lesion, 32 patients had their primary tumor at distal femur (69.6%), 10 at proximal tibia (21.8%), 1 at proximal fibula (2.2%), 1 patient at distal tibia, 1 at left iliac bone, and 1 at proximal humerus.

Eighteen patients (39.1%) presented with (PET/CT detected) metastatic deposits. Seven patients presented with lung metastases alone, six presented with nodal lesions alone, two presented with bone metastases alone, two patients presented with both lung and nodal lesions, and one patient presented with lung, bone, and nodal lesions. There were four patients presented with skipped lesions (8.7%).

According to histologic response to NAC, 14 patients were good responders (30.4%), with more than 90% tumor necrosis, while 31 patients were poor responders (67.4%). The results of one patient were missed.

Study parameters

The SUVmax1 of different pathological types in the studied 46 patients are reported in Table 1.

We noticed that the higher SUVmax1 was recorded by osteoblastic OS, while the lower SUVmax1 was recorded by chondroblastic OS.

Using one-way ANOVA test, we found that no statistically significant difference between different pathological types regarding SUVmax1 ($P = 0.611$).

Changes in magnetic resonance imaging tumor volume according to the pathological response

The change in MRTV was calculated for patients who underwent three MRI studies (31 patients) and patients underwent two studies only (1st and 2nd OR 1st and 3rd MRI) (14 patients). Regarding patients with three MRIs, there was significant increase of MRTV3 at poor responders group only ($P = 0.024$) [Figure 2]. While patients for whom only two MRIs were available, there was significant decrease of MRTV3 at good responders group only ($P = 0.016$).

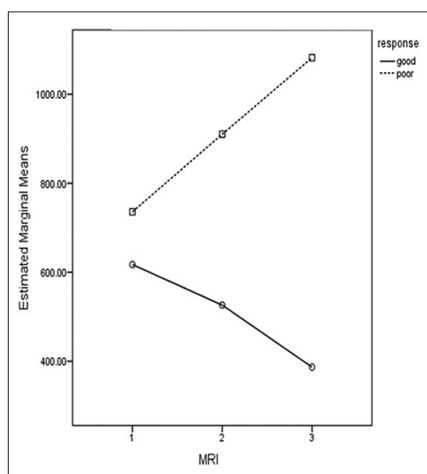


Figure 2: Changing in magnetic resonance imaging tumor volume in good and poor responders

Changes in positron emission tomography/computed tomography parameters according to the pathologic response

SUVmax and TLR are tested, patients for whom three PET/CTs were available (32 patients), the SUVmax2 and SUVmax3 showed significant decrease in comparison to baseline study for good responders group ($P = 0.003$) [Figure 3].

Patients for whom only two PET/CTs were available (8 patients had first and second studies and six patients had first and third studies), the SUVmax2 showed significant changes in comparison with baseline study for good responders and bad responders groups ($P = 0.003$ and 0.006 , respectively). Furthermore, SUVmax3 showed significant changes in comparison with baseline study for good responders and poor responders groups (both groups had $P = 0.001$). Patients for whom three PET/CTs were available, the TLR2 and TLR3 showed significant decrease in comparison with baseline study for good responders group ($P = 0.003, 0.001$) respectively.

While patients for whom only two PET/CTs were available, the TLR2 and TLR3 showed significant decrease in comparison with baseline study for good responders group with

Table 1: Maximum standardized uptake value 1 of the different pathological types

Pathological type	n	Mean	SD	Minimum	Maximum
Osteoblastic type	29	9.817	4.0028	3.4	19.4
Chondroblastic type	7	8.843	3.8262	3.2	13.4
Chondromyxoid type	1	7.300		7.3	7.3
MFH-like variant	2	11.600	1.1314	10.8	12.4
Osteoblastic/ chondroblastic variant	1	9.000		9.0	9.0
Fibroblastic type	1	17.000		17.0	17.0
Telangiectatic type	5	10.560	5.0088	6.0	18.0

MFH: Malignant fibrous histiocytoma; SD: Standard deviation

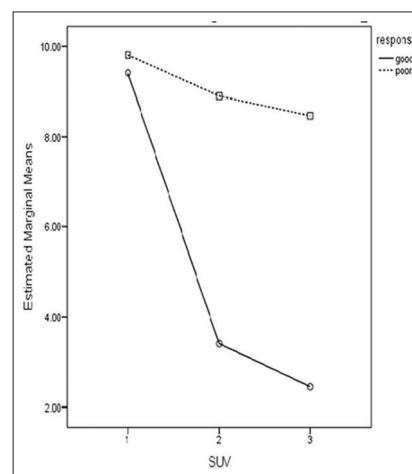


Figure 3: Changing in maximum standardized uptake value in good and poor responders

P value ($P = 0.001, 0.002$), respectively. Tables 2 and 3 show the mean, median, standard deviation, and Interquartile range of the SUVmax and MRTV values at good and poor responders.

Receiver operating characteristic curve analysis
Receiver operating characteristic curve analysis of standardized uptake value maximum 1 value

SUVmax1 proved to be of no value in predicting good or poor responders with area under curve (AUC) 0.594, so we cannot depend on SUVmax1 to predict aggressiveness of the disease.

Receiver operating characteristic curve analysis of maximum standardized uptake value 2 value

SUVmax2 proved to be excellent in predicting poor responders with AUC 0.984 (95% confidential interval [CI] 0.945–1). A cutoff value 4.25 defined at which SUVmax2 had a sensitivity of 92.3% and specificity of 92.3%. A lower cutoff value of 3.9 at which SUVmax2 had a higher sensitivity of 96.2% and lower specificity of 84.6%, while a higher cutoff value of 4.9 was defined at which SUVmax2 had a lower sensitivity of 84.6% and higher specificity of 100%. Values above these cutoff points predict poor response.

Receiver operating characteristic curve analysis of maximum standardized uptake value 2/1 ratio

The SUVmax2/1 proved to be excellent in predicting good and poor responders with SUVmax2/1 AUC 0.932 (95% CI 0.856–1.00), A cutoff value 0.41 was defined at which SUVmax2/1 had a sensitivity of 92.3% and specificity of 85% for predicting poor responders. Values above this cutoff predict poor response.

Table 2: Mean, median, standard deviation, and Interquartile range of maximum standardized uptake value values at good responders and poor responders groups

The parameter	Good responders				Poor responders			
	Mean	Median	IQR	SD	Mean	Median	IQR	SD
SUVmazx1	9.4	8.4	7.7-11.4	3	9.8	10.6	6.2-12.9	4
SUVmax2	3.4	3.5	3-3.9	0.66	9.8	8.5	6.6-10.7	3.4
SUVmax3	2.4	2.6	2-2.8	0.53	8.4	6.9	5.9-10.5	4.7

IQR: Interquarantine range; SD: Standard deviation; SUVmax: Maximum standardized uptake value

Table 3: Mean, median, standard deviation, and interquarantine range of MRTV values at good responders and poor responders groups

The parameter	Good responders			Poor responders				
	Mean	median	IQR	SD	Mean	median	IQR	SD
MRTV1	617.3	566.1	314.5-849.2	450.6	639.9	530.8	281.9-1157.4	423.4
MRTV2	526.1	417.6	212.7-879.8	385.1	823.7	627.6	470.4-1157.4	624.5
MRTV3	386.8	372.6	139.9-562.7	287.8	985.5	676	437.5-1480	1043.6

IQR: Interquartile range range; SD: Standard deviation; MRTV: Magnetic resonance tumor volume

Furthermore, ROC curve analysis of TLR2 value, TLR2/1 ratio, SUVmax3 value, SUVmax3/1 ratio, TLR3 value, and TLR3/1 ratio proved to be excellent in predicting poor responders.

While we found that ROC curve analysis of MRTV2/1 ratio and MRTV3/1 ratio was less efficient than the previous ratios in predicting poor responders.

Table 4 summarizes sensitivity and specificity of each PET/CT and MRI parameters.

A higher sensitivity for detecting poor responders was detected by SUVmax3/1, TLR3/1, and MRTV2/1 cutoff values, while a higher specificity was detected by TRL2 and SUVmax3 cutoff values.

PET/CT and MRI images of four OS cases with different response to neoadjuvant chemotherapy are shown in Figures 4a-f, 5a-e, 6a-f, and 7a-e.

DISCUSSION

It is essential to monitor the response to chemotherapy to determine whether the prescribed treatment regimen is effective or not. Treatment response is considered to be successful if, histologically, more than 90% of tumor cells show necrosis,^[11] which has been reported to be the most important prognostic factor for disease control and only can be evaluated after completion of neoadjuvant chemotherapy.^[12]

However, because tumor necrosis can have assessed only in the resected specimens after the completion of neoadjuvant chemotherapy, the continuation of ineffective chemotherapy can cause the development of resistant clones.^[13]

Unlike morphologic imaging modalities, ¹⁸F-FDG-PET reflects the metabolic rate of glycolysis in tumors, and thus, ¹⁸F-FDG-PET should be more accurate for assessing treatment response because it can more correctly identify viable residual tumors.^[14]

In this prospective study, we found that 39.1% of patients had metastatic deposits at the initial presentation and 8.7% of patients had skip lesions (four patients) at the initial presentation.

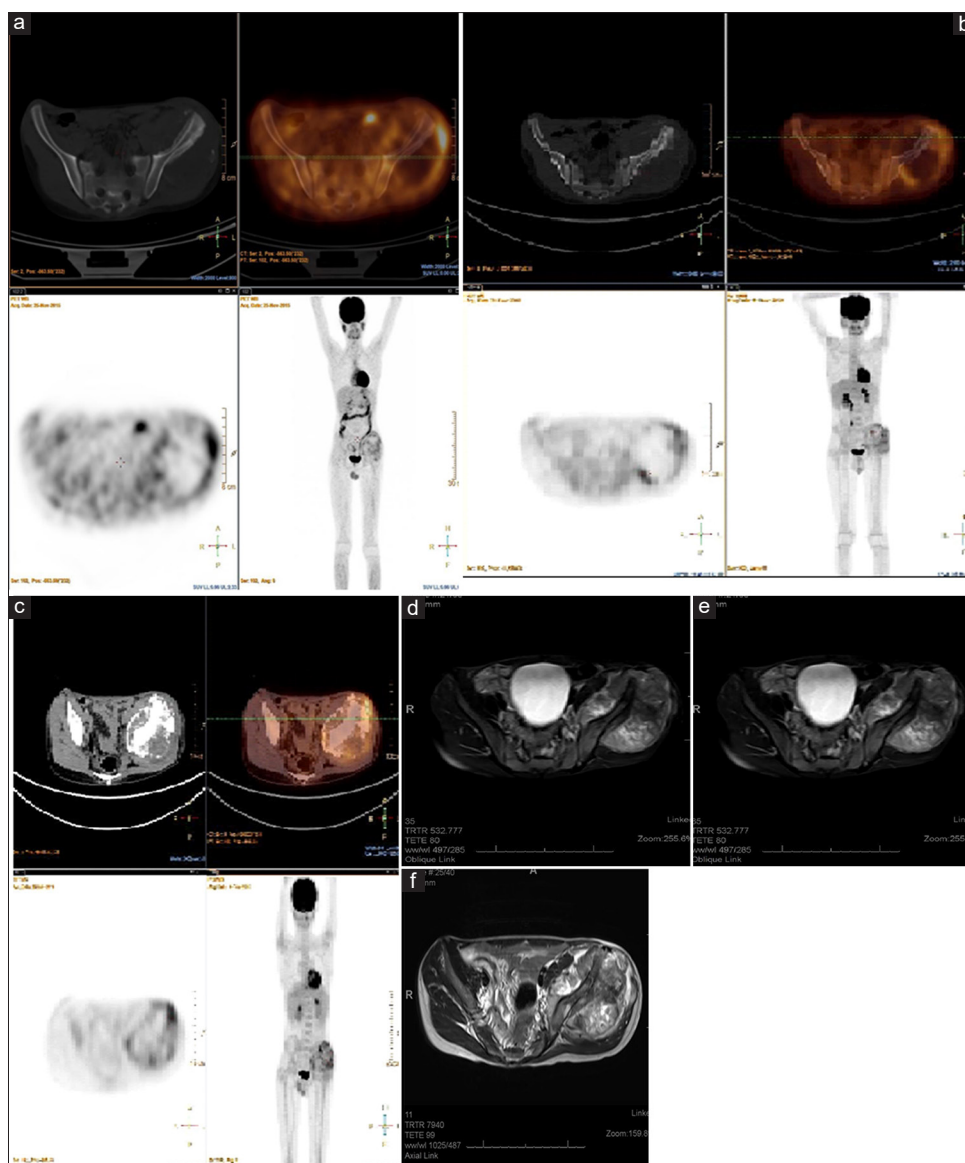


Figure 4: A 14-year-old male patient suffered from left iliac bone high-grade conventional osteosarcoma chondroblastic variant. The surgical pathology revealed poor histological response (36% tissue necrosis). Positron emission tomography computed tomography and magnetic resonance imaging parameters of the first case: in maximum standardized uptake value 1 = 3.2, in maximum standardized uptake value 2 = 4.1, in maximum standardized uptake value 2/1 = 1.28, tumor liver ratio 2 = 1.86, tumor liver ratio 2/1 = 1.28, maximum standardized uptake value 3 = 5.6, maximum standardized uptake value 3/1 = 1.75, TRL3 = 2.33, TRL3/1 = 1.6, magnetic resonance imaging tumor volume 2/1 = 1, magnetic resonance imaging tumor volume3/1 = 1. (a) First positron emission tomography computed tomography of the first case. (b) Second positron emission tomography-computed tomography of the first case. (c) Third positron emission tomography/computed tomography of the first case. (d) First magnetic resonance imaging of the first case. (e) Second magnetic resonance imaging of the first case. (f) Third magnetic resonance imaging of the first case

Among the studied patients, 30.4% showed a good histologic response in the resected specimens after neoadjuvant chemotherapy.

Similar to our results, Byun *et al.* in their study, which was conducted on 30 patients with OS, stated that 44% of the patients were good responders.^[15]

This difference in the percentage of patients who presented with metastatic disease may be due to late referral of OS patients to specialized oncology centers in Egypt (CCHE) that

may have contributed also to the difference in the percentage of good responders to the NAC.

Our study had several important findings. First, we found that ¹⁸F-FDG-PET/CT performed after 3 cycles of NAC is useful to predict a poor histologic response as well as following completion of NAC (post-6 cycles) in patients with OS. Second, PET/CT parameters are capable of predicting histological response with overall sensitivity and specificity higher than MRTV parameters, which can be explained by several possible causes. The first is the slow regression of the

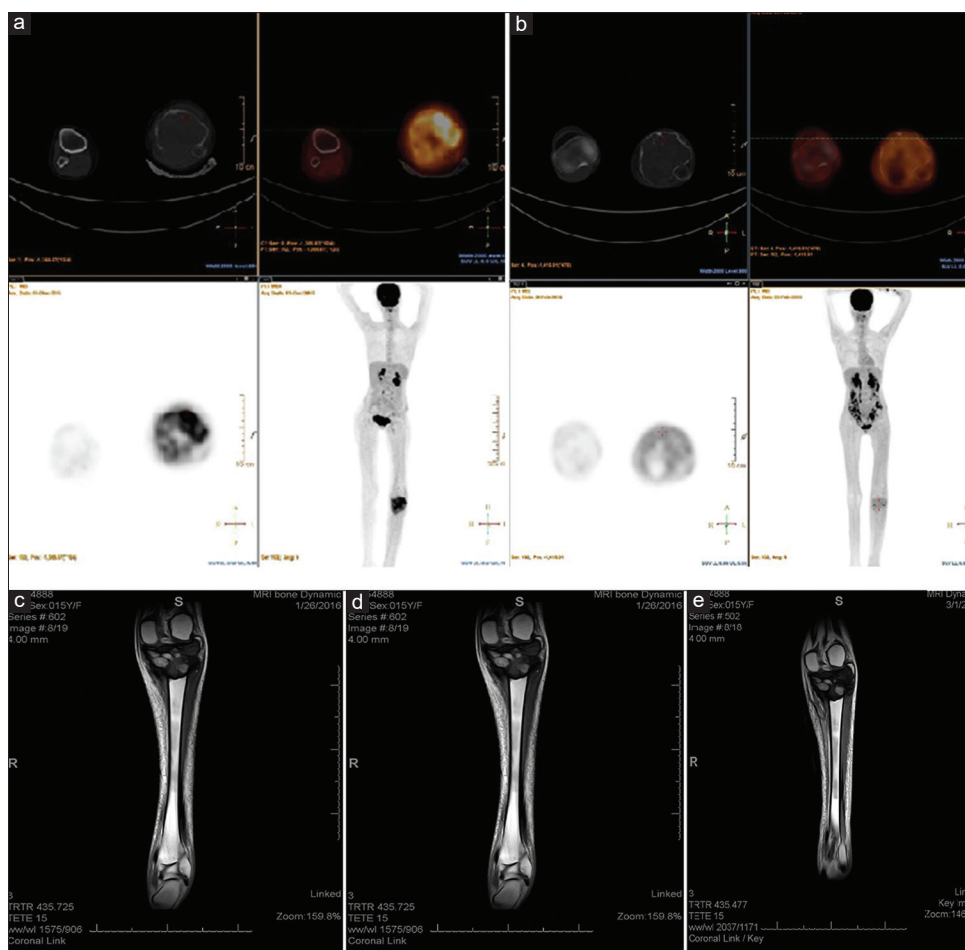


Figure 5: A 14-year-old female patient suffered from left proximal tibia telangiectatic osteosarcoma. The surgical pathology revealed good histological response (100% tissue necrosis). Positron emission tomography/computed tomography and MRI parameters of the second case: maximum standardized uptake value 1 = 12.4, maximum standardized uptake value 2 = 2.6, maximum standardized uptake value 2/1 = 0.21, tumor liver ratio 2 = 0.92, tumor liver ratio 2/1 = 0.14, maximum standardized uptake value 3 = 1.8, maximum standardized uptake value 3/1 = 0.15, TRL3 = 0.94, TRL3/1 = 0.15, magnetic resonance imaging tumor volume 2/1 = 1.47, magnetic resonance imaging tumor volume 3/1 = 0.89. (a) first positron emission tomography/computed tomography of the second case. (b) Second positron emission tomography/computed tomography of the second case. (c) Third positron emission tomography/computed tomography of the second case. (d) Second magnetic resonance imaging of the second case. (e) Third magnetic resonance imaging of the second case

Table 4: Sensitivity and specificity of different parameter's cutoff values

Tested parameter	Cutoff value above which bad responders were suggested (%)	Sensitivity	Specificity
SUVmax2	4.25	92.3	92.3
SUVmax2/1	0.41	92.3	85
TLR2	2.6	80.8	100
TLR2/1	0.39	92.3	73.1
SUVmax3	3.5	91.7	100
SUVmax3/1	0.44	100	83.3
TLR3	1.31	95.8	91.7
TLR3/1	0.49	100	79.2
MRTV2/1	0.73	100	30.8
MRTV3/1	0.056	83.3	46

TLR: Tumor liver ratios; SUVmax: Maximum standardized uptake value; MRTV: Magnetic resonance imaging tumor volume

osteoid matrix and cystic degeneration in good responders with a corresponding fallacious increase in MRTV.^[16] Second, the MRTV calculated using the multiplication of the three dimensions of the tumor size does not represent the real tumor burden containing necrotic portions with nonviable tissue.

According to the PET/CT parameters, we found that SUVmax values had overall sensitivities and specificities higher than those of TLRs.

Regarding cutoff values that were calculated by ROC curve analysis of the second PET/CT parameters (post three cycles of NAC), we concluded that SUVmax2/1 more than 0.4 could predict poor responders with sensitivity and specificity 92.3% and 85%, respectively, and SUVmax2 more

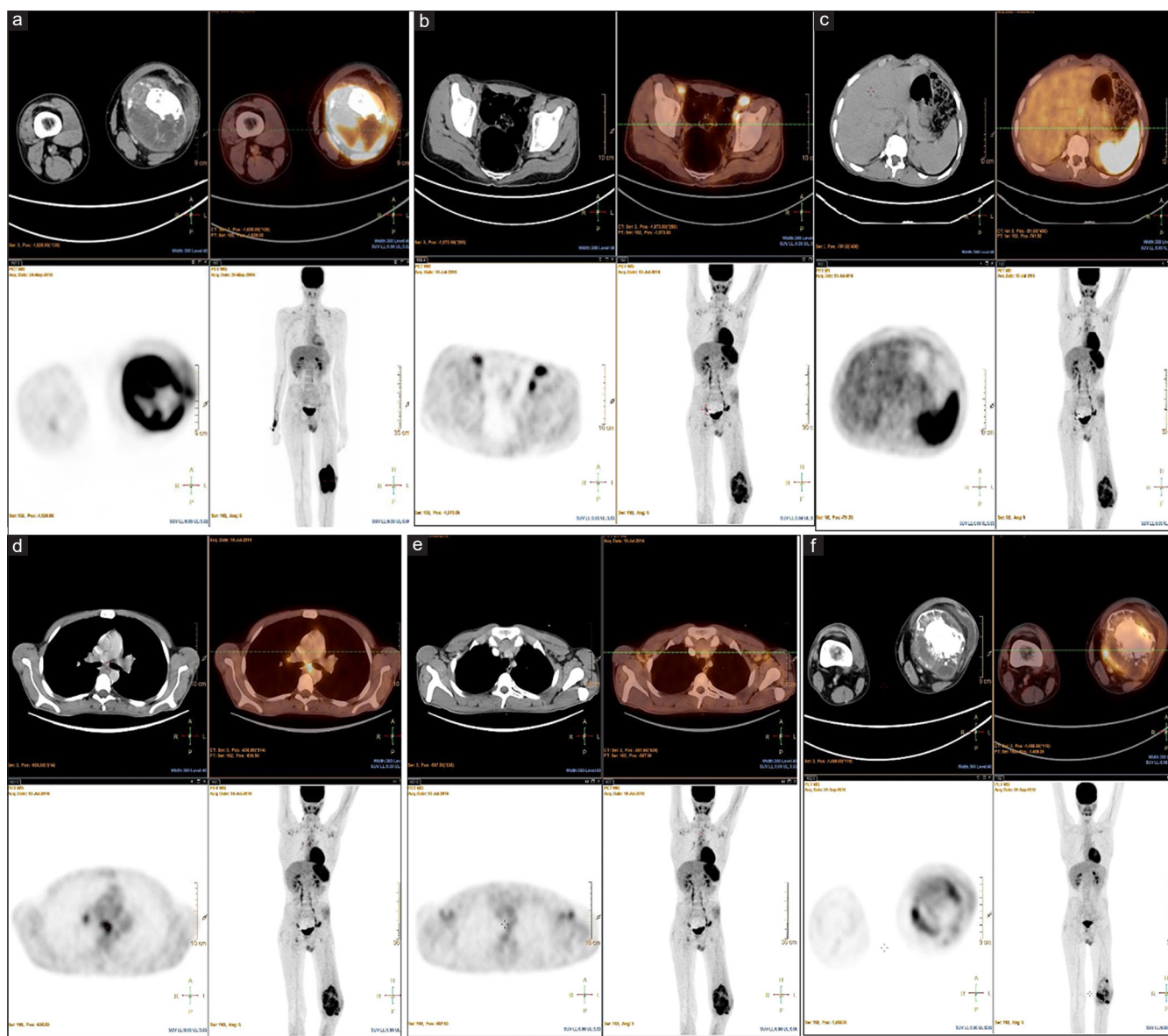


Figure 6: A 17-year-old male patient had left lower femur osteosarcoma. The first positron emission tomography/computed tomography detected solitary left external iliac lymph node with maximum standardized uptake value less than the reference hepatic activity. At second positron emission tomography/computed tomography, multiple fluorodeoxyglucose avid nodal lesions involving cervical, axillary, mediastinal, and abdominal–pelvic regions and diffuse splenic fluorodeoxyglucose uptake were detected, fine needle aspiration cytology from cervical lymph nodes revealed scanty lymphoid tissue with no evidence of atypical or malignant cells. At the third positron emission tomography/computed tomography, complete metabolic regression of all nodal lesions was noted. (a) Second positron emission tomography/computed tomography of the third case. (b) Second positron emission tomography/computed tomography showed fluorodeoxyglucose avid pelvic lymph nodes. (c) Second positron emission tomography/computed tomography showed diffuse splenic fluorodeoxyglucose FDG uptake. (d) Second positron emission tomography/computed tomography showed fluorodeoxyglucose avid mediastinal lymph nodes. (e) Second positron emission tomography/computed tomography showed fluorodeoxyglucose avid axillary lymph nodes. (f) Third positron emission tomography/computed tomography showed complete resolution of fluorodeoxyglucose lesions

than 4.25 could predict poor responders with sensitivity 92.3% and specificity 92.3%. In addition, SUVmax3/1 less than 0.44 (–56% ΔSUV) could predict good responders with sensitivity and specificity 100% and 83.3%, respectively. SUVmax3 less than 3.5 could predict good responders with sensitivity 91.7% and specificity 100%. We also found that MRTV2/1 cutoff value of 0.73 could predict poor responders

above this value with 100% sensitivity and 30.8% specificity, while MRTV3/1 cutoff value of 0.056 could predict poor responders above this value with 83.3% sensitivity and 46% specificity.

However, we found that SUVmax1 to be of no value in predicting good or poor responders with AUC 0.594, so we

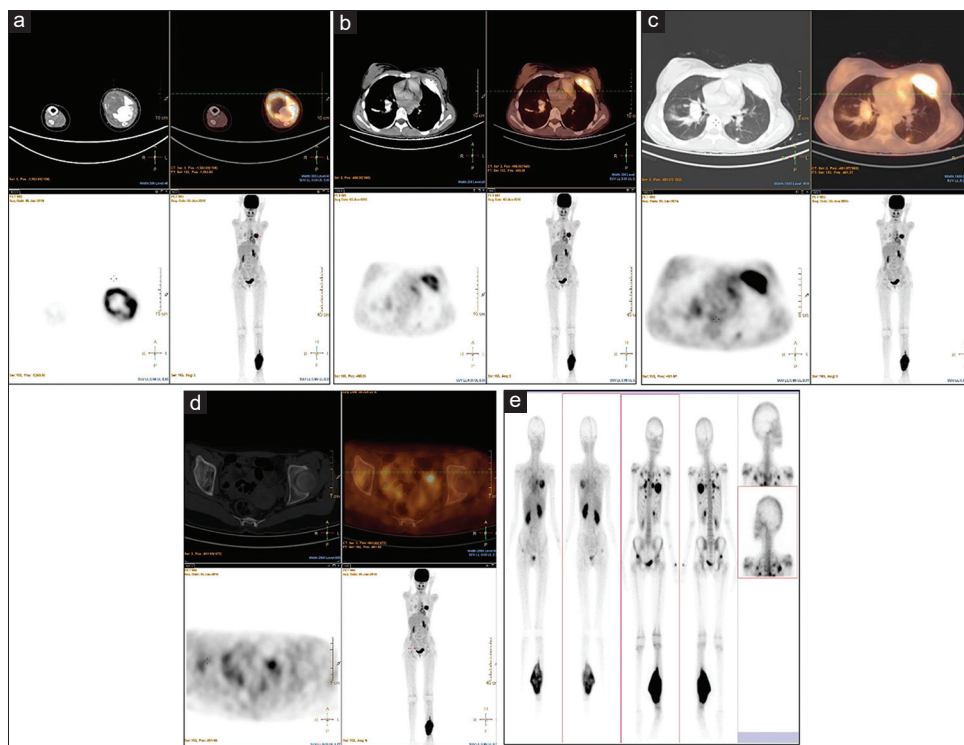


Figure 7: A 14-year-old female patient suffered from left distal tibia conventional osteosarcoma, osteoblastic variant (high grade). At the first positron emission tomography/computed tomography scan, we detected fluorodeoxyglucose avid metastatic osseous and lung deposits as well as fluorodeoxyglucose nodal lesions. Positron emission tomography/computed tomography could detect the metastatic osseous deposits, which were seen at the bone scan. The second and third positron emission tomography/computed tomography scan showed stationary course of the disease with no improvement. (a) First positron emission tomography/computed tomography of the fourth case. (b) Positron emission tomography/computed tomography of the fourth case showed metastatic fluorodeoxyglucose avid left-sided destructive rib lesion. (c) Positron emission tomography/computed tomography of the fourth case showed fluorodeoxyglucose lung deposits. (d) Positron emission tomography/computed tomography of the fourth case showed fluorodeoxyglucose avid metastatic right acetabular lesion. (e) Bone scan of the fourth case showed the primary osteosarcoma, bone, and calcified lung deposits

cannot depend on SUVmax1 to predict aggressiveness of the disease.

Byun *et al.* tested initial PET/MR parameters and proved that none of these parameters can predict a poor histologic response.

In addition, they found that SUVmax1 (after three cycles of NAC) above cutoff value of six could predict poor responders with 88% sensitivity and 54% specificity.

They also concluded that SUVmax2 (after six cycles of NAC) above cutoff value of five could predict poor responders with 59% sensitivity and 92% specificity. Similar to our results, they found that MR tumor volume cutoff values to be of low sensitivity and specificity in this consideration.^[17]

Hyung *et al.* evaluated twenty patients of OS. All patients underwent ¹⁸F-FDG-PET/CT scans before and after neoadjuvant chemotherapy. In their study, ROC curve analysis of the second PET/CT parameters (post-3 cycles of NAC), showed that, SUVmax2/1 more than 0.65 could predict poor responders with sensitivity and specificity of 80% and 88.9% respectively,

SUVmax2 (after three cycles of NAC) above cutoff value of 3.2 could predict poor responders with 100% sensitivity and 88.9% specificity. SUVmax3/1 less than 0.48 could predict good responders with sensitivity and specificity 80% and 77.8%, respectively; while SUVmax3 (after 6 cycles of NAC) above cutoff value of three could predict poor responders with 100% sensitivity and 88.9% specificity,^[6] these results were comparable to ours.

Very recent studies evaluating the usefulness of SUV in predicting response to neoadjuvant chemotherapy had shown that post- to pre-therapy SUVmax ratio and posttherapy SUVmax correlated with histological response.^[18]

Several studies have suggested reduction about – 60% to –40% of (SUVmax3/1) as the cutoff value for good response to neoadjuvant chemotherapy of OS.^[19] Cheon *et al.* found that patients with an SUV2 (after completion of NAC) of less than or equal to 2 showed a good histologic response with accuracy of 63%, and patients with an SUV2 >5 showed a poor histologic response with accuracy of 84%.^[20]

Kong *et al.* defined prechemotherapy SUVmax as SUV1 and preoperative SUVmax as SUV2. They found that SUVmax2 cutoff more than 5 had predicted poor responders with a sensitivity of 61.5% and a specificity of 92.3%.^[21]

Future prospective multicenter trials are needed to address whether PET and MRI parameters can provide prognostic information similar or superior to that provided by the histologic response after the completion of NAC. This future study would provide the rationale for clinicians to decide whether NAC should be continued or discontinued based on PET/CT and MRI parameters after week 5 and 10 of NAC.

CONCLUSION

¹⁸F-FDG-PET/CT performed after 3 cycles of NAC is useful to predict a poor histologic response as well as following completion of NAC (postweek 10) in patients with OS. PET/CT parameters are capable of predicting histological response with overall sensitivity and specificity higher than MRTV parameters.

Financial support and sponsorship

Nil.

Conflicts of interest

There are no conflicts of interest.

REFERENCES

1. Marulanda GA, Henderson ER, Johnson DA, Letson GD, Cheong D. Orthopedic surgery options for the treatment of primary osteosarcoma. *Cancer Control* 2008;15:13-20.
2. Rosen G, Forscher CA, Mankin HJ, Selch MT; Bone Tumors. In *Holland-Frei Cancer Medicine*. Bast RC, Kufe DW, Pollock RE, Wechselbaum RR, Gansler TS, Holland JF *et al.*, editors; 5th edition, Hamilton (ON): BC Decker; 2000. p. 8.
3. Link MP, Goorin AM, Miser AW, Green AA, Pratt CB, Belasco JB, *et al.* The effect of adjuvant chemotherapy on relapse-free survival in patients with osteosarcoma of the extremity. *N Engl J Med* 1986;314:1600-6.
4. Picci P. Osteosarcoma (osteogenic sarcoma). *Orphanet J Rare Dis* 2007;2:6.
5. Miwa S, Shirai T, Taki J, Sumiya H, Nishida H, Hayashi K, *et al.* Use of ^{99m}Tc-MIBI scintigraphy in the evaluation of the response to chemotherapy for osteosarcoma: Comparison with ²⁰¹Tl scintigraphy and angiography. *Int J Clin Oncol* 2011;16:373-8.
6. Im HJ, Kim TS, Park SY, Min HS, Kim JH, Kang HG, *et al.* Prediction of tumour necrosis fractions using metabolic and volumetric ¹⁸F-FDG PET/CT indices, after one course and at the completion of neoadjuvant chemotherapy, in children and young adults with osteosarcoma. *Eur J Nucl Med Mol Imaging* 2012;39:39-49.
7. Benjamin RS, Choi H, Macapinlac HA, Burgess MA, Patel SR, Chen LL, *et al.* We should desist using RECIST, at least in GIST. *J Clin Oncol* 2007;25:1760-4.
8. Schuetze SM, Baker LH, Benjamin RS, Canetta R. Selection of response criteria for clinical trials of sarcoma treatment. *Oncologist* 2008;13 Suppl 2:32-40.
9. Kim SY, Helman LJ. Strategies to explore new approaches in the investigation and treatment of osteosarcoma. *Cancer Treat Res* 2009;152:517-28.
10. Bacci G, Longhi A, Fagioli F, Briccoli A, Versari M, Picci P, *et al.* Adjuvant and neoadjuvant chemotherapy for osteosarcoma of the extremities: 27 year experience at Rizzoli institute, Italy. *Eur J Cancer* 2005;41:2836-45.
11. Uhl M, Saueressig U, Koehler G, Kontny U, Niemeyer C, Reichardt W, *et al.* Evaluation of tumour necrosis during chemotherapy with diffusion-weighted MR imaging: Preliminary results in osteosarcomas. *Pediatr Radiol* 2006;36:1306-11.
12. Davis AM, Bell RS, Goodwin PJ. Prognostic factors in osteosarcoma: A critical review. *J Clin Oncol* 1994;12:423-31.
13. Bajpai J, Gamnagatti S, Kumar R, Sreenivas V, Sharma MC, Khan SA, *et al.* Role of MRI in osteosarcoma for evaluation and prediction of chemotherapy response: Correlation with histological necrosis. *Pediatr Radiol* 2011;41:441-50.
14. Schulte M, Brecht-Krauss D, Werner M, Hartwig E, Sarkar MR, Keppler P, *et al.* Evaluation of neoadjuvant therapy response of osteogenic sarcoma using FDG PET. *J Nucl Med* 1999;40:1637-43.
15. Byun BH, Kong CB, Lim I, Choi CW, Song WS, Cho WH, *et al.* Combination of ¹⁸F-FDG PET/CT and diffusion-weighted MR imaging as a predictor of histologic response to neoadjuvant chemotherapy: Preliminary results in osteosarcoma. *J Nucl Med* 2013;54:1053-9.
16. van der Woude HJ, Bloem JL, Hogendoorn PC. Preoperative evaluation and monitoring chemotherapy in patients with high-grade osteogenic and Ewing's sarcoma: Review of current imaging modalities. *Skeletal Radiol* 1998;27:57-71.
17. Byun BH, Kong CB, Lim I, Kim BI, Choi CW, Song WS, *et al.* Early response monitoring to neoadjuvant chemotherapy in osteosarcoma using sequential ¹⁸F-FDG PET/CT and MRI. *Eur J Nucl Med Mol Imaging* 2014;41:1553-62.
18. Ye Z, Zhu J, Tian M, Zhang H, Zhan H, Zhao C, *et al.* Response of osteogenic sarcoma to neoadjuvant therapy: Evaluated by ¹⁸F-FDG-PET. *Ann Nucl Med* 2008;22:475-80.
19. Hawkins DS, Conrad EU 3rd, Butrynski JE, Schuetze SM, Eary JF. [¹⁸F]-fluorodeoxy-D-glucose-positron emission tomography response is associated with outcome for extremity osteosarcoma in children and young adults. *Cancer* 2009;115:3519-25.
20. Cheon GJ, Kim MS, Lee JA, Lee SY, Cho WH, Song WS, *et al.* Prediction model of chemotherapy response in osteosarcoma by ¹⁸F-FDG PET and MRI. *J Nucl Med* 2009;50:1435-40.
21. Kong CB, Byun BH, Lim I, Choi CW, Lim SM, Song WS, *et al.* ¹⁶⁷F-FDG PET SUVmax as an indicator of histopathologic response after neoadjuvant chemotherapy in extremity osteosarcoma. *Eur J Nucl Med Mol Imaging* 2013;40:728-36.